Homologous recombination deficiency serves as a prognostic biomarker in clear cell renal cell carcinoma

LIPING HE[1*], FENG GAO[1*], JINGYU ZHU[1*], QIAOPING XU[2*], QIQI YU[1], MEI YANG[1] and YASHENG HUANG[1]

[1]Department of Urology, Hangzhou Hospital of Traditional Chinese Medicine, Hangzhou, Zhejiang 310007; [2]Department of Clinical Pharmacology, Key Laboratory of Clinical Cancer Pharmacology and Toxicology Research of Zhejiang Province, Affiliated Hangzhou First People's Hospital, Cancer Center, Zhejiang University School of Medicine, Hangzhou, Zhejiang 310000, P.R. China

Received October 21, 2022; Accepted April 18, 2023

DOI: 10.3892/etm.2023.12128

Abstract. Kidney renal clear cell carcinoma (KIRC) is a frequent malignant tumor characterized by a high degree of heterogeneity and genetic instability. DNA double-strand breaks generated by homologous recombination deficit (HRD) are a well-known contributor to genomic instability, which can encourage tumor development. It is not known, however, whether the molecular characteristics linked with HRD have a predictive role in KIRC. The discovery cohort comprised 501 KIRC patients from The Cancer Genome Atlas database. Genome and transcriptome data of HRD patients were used for comprehensive analysis. Single cell RNA sequencing (scRNA-seq) was used to verify the test results of bulk RNA-seq. In the present study, patients with a high HRD score had a worse prognosis compared with those with a low HRD score. The DNA damage response signaling pathways and immune-related signaling pathways were notably enriched in the HRD-positive subgroup. Further comprehensive analysis of the tumor microenvironment (TME) revealed that the signal of exhausted CD8+ T cells was enriched in the HRD-positive subgroup. Finally, scRNA-seq analyses confirmed that the immune-related signaling pathways were upregulated in HRD-positive patients. In conclusion, the present study not only demonstrated that a high HRD score is a valid prognostic biomarker in KIRC patients, but also revealed the TME in HRD-positive tumors.

Correspondence to: Professor Yasheng Huang, Department of Urology, Hangzhou Hospital of Traditional Chinese Medicine, 453 Tiyuchang Road, Hangzhou, Zhejiang 310007, P.R. China
E-mail: huangyasheng022@126.com

*Contributed equally

Key words: homologous recombination deficit, single cell RNA sequencing, tumor microenvironment

Introduction

Renal cell carcinoma (RCC) is a prevalent urologic malignancy with incidence and fatality rates that rank fifteenth among malignant tumors (1). RCC is divided histologically into subtypes, with kidney renal clear cell carcinoma (KIRC) accounting for >80% of RCCs, followed by papillary RCC and chromophobe RCC (2,3). Despite the fact that KIRC is a disease that may be detected early and successfully treated with surgical or ablative techniques, up to one-third of cases will present with or acquire metastases and 20-40% of cases will relapse after nephrectomy for localized disease (4). KIRC is particularly resistant to chemotherapy and the conventional treatment for metastatic KIRC5 is targeted therapy with tyrosine kinase inhibitor (TKI)/mammalian target of rapamycin inhibitor (mTORi) with or without immunotherapy (5). Once KIRC recurs, no additional treatment is successful.

The majority of patients with KIRC demonstrate chromosomal 3p deletion and genomic mutations in the Von Hippel-Lindau (VHL) Tumor Suppressor allele (6), followed by secondary loss of several tumor suppressor genes, such as *PBRM1, SETD2, BAP1* and/or *KDM5C* (7). These genes also contribute to genomic instability (8).

Additionally, a significant contributor to genomic instability is homologous recombination repair deficiency (HRD) (9). As a potent prognostic biomarker, HRD has been discovered in recent years in a number of types of cancer. Although identification of HRD in adrenal cortical carcinoma predicts a worse clinical prognosis compared with non-HRD patients, molecular characterization of HRD in ovarian malignancies predicts more effective PARP inhibitor therapy and longer life (10). The current clinical detection of HRD is theoretically based on the specific, quantifiable and permanent genomic alterations produced by HRD, such as identifying genetic mutations, insertion/deletion patterns, chromosomal structural abnormalities and gene copy number variations (11). A 'genomic scar' made up of large-scale state transitions (LST), telomere allele imbalance (TAI) and genomic heterozygosity loss (LOH) may result from HRD, a functional defect in homologous recombinant DNA repair (12). The HRD state of cells can be partially described by LOH, TAI and LST, each of which have unique definitions. The HRD score,

which is created from the three markers (LOH+TAI+LST), is a more reliable predictor of HRD than any of the individual scores, even though each score has clinical significance on its own (13,14). The relationship between HRD and tumors has been extensively studied in other types of cancer, such as ovarian cancer and breast cancer, but it is still unclear how HRD affects the prognosis and the tumor microenvironment (TME) in KIRC (15,16).

The present study discovered that HRD was a prognostic indicator for patients with clear cell renal cell carcinoma. HRD patients exhibited a characteristic upregulation of immune-related and DNA damage repair pathways. Single cell RNA sequencing (scRNA-seq) analysis revealed a higher prevalence of exhausted T cell signatures in patients with HRD. The present study is expected to yield novel insights into the individualized treatment of KIRC.

Materials and methods

Sample collection. In the present study, four KIRC patients with HRD-positive tumors were recruited between March 2021 and June 2021 in Hangzhou Hospital of Traditional Chinese Medicine (Table SI). For KIRC patients, tumor tissues, adjacent normal tissues were collected. Written informed consent was obtained from all participants. The present study was performed in accordance with the ethical principles of the Declaration of Helsinki and was approved by the Research and Ethics Committee of Hangzhou Hospital of Traditional Chinese Medicine (approval no. 2019KY005). The patients underwent next-generation sequencing using whole exome sequencing (WES). Using matched normal (blood) samples from each patient as a reference, tumor mutation burden (TMB) was computed as the total detected missense mutations in the pretreatment tumor samples (17). PD-L1 expression on tumor cells was prospectively assessed using the Dako PD-L1 IHC 28-8 pharmDx test (Agilent Technologies, Inc.) (18). Microsatellite instability is calculated using the MSIsensor algorithm (19).

Data collection and processing. The Cancer Genome Atlas (TCGA) database, which is open to the public and can be accessed at https://portal.gdc.cancer.gov, was used to download the Original WES sequencing data, gene expression profile data and associated clinical follow-up data (20). From the TCGA databases, 501 KIRC samples with complete clinical data were obtained (https://www.cbioportal.org/study/clinicalData?id=kirc_tcga_pan_can_atlas_2018). VarScan2 was used to identify somatic mutations, such as insertion-deletions and single nucleotide polymorphisms (21). Synonymous single nucleotide variants (SNV), non-synonymous SNV, stop gain SNV, non-frameshift insertions and frameshift deletions were among the exonic alterations that were extracted from the mutation points and annotated using ANNOVAR (22). The cBioPortal database (https://www.cbioportal.org/study/summary?id=kirc_tcga_pan_can_atlas_2018) provided the somatic mutation counts, copy number variation (CNV), fraction genome altered scores (FGA; percentage of copy number altered chromosome regions out of measured regions) and TMB sensor score (tumor mutation burden detection using paired tumor-normal sequence data) (23). Lymphocytes infiltrating HRD and homologous recombination proficient (HRP) tumors were obtained from public database (https://doi.org/10.5522/04/16573640.v1) (24).

HRD score analysis. The number of counts of chromosomal LOH regions longer than 15 Mb but shorter than the entire chromosome was used to define loss of heterozygosity (LOH) (25). After smoothing and filtering out small-scale copy number variation shorter than 3 Mb, LST were defined as chromosome breakpoints (change in copy number or allelic content) between adjacent regions, each of ≥10 Mb (26). The quantity of regions with allelic imbalance that reach the sub-telomere but do not cross the centromere is known as telomeric allelic imbalance (TAI) (27). The TAI, LST and LOH scores were added together to create the HRD score. Table SII displays each patient's HRD score.

Difference analysis and enrichment analysis. Using the R-package (https://www.r-project.org/) DEseq2 (28), the differences between various molecular subtypes were examined. The cutoffs to find differentially expressed genes (DEGs) were set as fold change >1 and adj. $P<0.05$. For the HRD group, the present study used gene ontology (GO) enrichment analysis to identify specific biological functions. All peak-related genes were first assigned to GO terms in the GO database. Gene numbers were calculated for each term and a hypergeometric test was used to identify GO terms that were significantly enriched in peak-related genes compared with the genome background. Additionally, the reference gene set for gene set enrichment analysis (GSEA; cp.kegg.v7.0.symbols.gmt) was used to examine the enrichment of various molecular subtypes in various pathways (29). $P<0.05$ and a false discovery rate (FDR) threshold of 0.25 were used to determine which pathways were significantly enriched.

scRNA-seq data processing and quality control. Mammary tissues from both benign and malignant tumors were saved during surgery and processed in 1 h using Tissue Storage Solution (Miltenyi Biotec GmbH). Following being rinsed in PBS, samples were mechanically separated using a razor blade. Dissociated samples were processed in RPMI Medium 1640 (Gibco; Thermo Fisher Scientific, Inc.) with collagenase/hyaluronidase (20%; Stemcell Technologies, Inc.) and BSA (20 mg/ml; Beijing Solarbio Science & Technology Co., Ltd.) at 37˚C for 1 h in order to produce cell suspensions. In order to create single-cell suspensions, the cells were next rinsed in a cold Hank's balanced salt solution (Beijing Solarbio Science & Technology Co., Ltd.) containing 0.04 percent BSA. The 10x Genomic Chromium Next GEM Single Cell 5' Reagents kit V2 (dual index) (10x Genomics) was used to create a 5'gene expression library. Using the High Output kit v2.5 and the NextSeq (Illumina, Inc.), the samples were sequenced (150 Cycles). The aggregated scRNA-seq library's low-quality cells were eliminated (500 <nFeature <10,000; 1000 <nCount <100,000 and 0 <pMT <0.2). Datasets were subsequently preprocessed with DoubletFinder v2.0.2 (30) to eliminate heterotypic doublets (presuming 6% of barcodes are doublets). With SCTransform and Harmony (31), the filtered library was normalized and batch effects were removed. Cell distances were then visualized in a reduced two-dimensional space using the t-distributed stochastic neighbor embedding

or uniform manifold approximation and projection (UMAP) method (https://satijalab.org/seurat/reference/runumap). scType was used to conduct cell type annotation and the cell markers used in this work were taken from earlier studies (Table SIII) (32). DEseq2 was used to determine the significance of each gene (FDR <0.01; fold change |log2FC| >1) in order to find the DEGs between two groups of clusters.

Single-cell copy-number variation (CNV) evaluation. The inferCNV R package (version 1.4.0; https://github.com/broadinstitute/inferCNV/wiki) was used to evaluate the CNV of each cell. The CNVs of cells with renal cell carcinoma were calculated, using stromal cells as the standard. The default hidden Markov model (HMM) settings, 'denoise' and a value of 0.1 for cutoff were used in the inferCNV analysis. The default Bayesian latent mixture model was used to identify the posterior probabilities of the CNV alterations in each cell with the default value of 0.5 as the threshold in order to decrease the number of false-positive CNV calls.

Data and code availability. The single cell datasets and code generated during the present study are accessible in the Zenodo database (https://zenodo.org/record/7783618#.ZCTwZXZBy3A).

Results

Genomic scar-based homologous recombination deficit (HRD) scores and prognostic analysis in KIRC. The discovery cohort of the present study included 501 KIRC patients from TCGA database to examine the potential relevance of HRD in KIRC. The top 20% of patients with the highest HRD scores and the bottom 20% of patients with the lowest HRD scores were determined using WES data for each KIRC sample and these samples were then sorted based on HRD scores. In terms of overall survival (OS; log-rank test; P=0.0004), disease-specific survival (DSS; log-rank test; P=0.15), or disease progression-free survival (PFS; log-rank test; P=0.0008), patients with HRD had a worse prognosis compared with patients with HRP, according to the results of the survival analysis (Fig. 1A).

The present study examined genome-wide copy number variation to show differences in genomic instability between HRD and HRP patients because HRD is an assessment of genome-wide traces. As expected, HRD patients had more genomic instability (Fig. 1B).

The mutation landscape in KIRC. An integrated analysis of the WES data was conducted in the study population (The top 20% of patients with the highest HRD scores and the bottom 20% of patients with the lowest HRD scores). The five most frequently mutated genes, *VHL, PBRM1, TTN, SETD2* and *BAP1*, all displayed mutation rates of >15% in both groups, as shown in Fig. 2A, which was consistent with the findings of other cohort studies. Next, the additional genetic variations between the two categories was assessed, including mutation count and fraction genome altered (FGA). In the HRD group compared with the HRP group, the signs of genomic instability were significantly more prevalent (Wilcoxon signed-rank test, P<0.0001, Fig. 2B).

Discovering the HRD transcriptome signature in KIRC. To explore the transcriptomic signatures associated with HRD, the KIRC gene expression profile data was examined to understand HRD-specific transcriptome markers (Fig. 2C). A total of 1,540 genes were found to be differentially expressed between HRD and HRP patients according to the DEseq2 analysis of gene expression profiling data (|logFC| >1.5; FDR 0.05). Specifically, out of the 1,540 DEGs, 630 DEGs were upregulated and 910 were downregulated (Fig. 3A). Using the online analytical tool DAVID, Kyoto Encyclopedia of Genes and Genomes (KEGG) signaling pathway enrichment analysis and Gene Ontology (GO) functional annotation were performed to obtain a thorough and in-depth understanding of the biological characteristics of these DEGs. According to GO analysis, sister chromatid cohesion, mitotic nuclear division, inflammatory response and other biological processes are among the enriched biological processes (BP) of upregulated DEGs. The enriched molecular function (MF) of upregulated DEGs included chemokine activity, DNA replication origin binding and anaphase-promoting complex binding (Fig. 3B). The regulation of lipolysis in adipocytes, aldosterone synthesis and secretion, GABAergic synapses, vascular smooth muscle contraction, chemokine signaling pathway and Chemokine-Chemokine receptor interaction are among the enriched pathways of upregulated DEGs, according to KEGG analysis (Fig. 3B). The homologous recombination pathway, the base-excision repair pathway, Chemokine receptor interaction and the cytosolic DNA sensing pathway were all significantly enriched in the HRD group, according to the GSEA analysis (Fig. 3C).

Analysis of tissue samples from HRD-positive KIRC patients using single-cell sequencing. As standard bulk RNA-sequencing assumes that each gene is expressed identically in every cell (33), it is obviously unable to explore intratumoral heterogeneity at the cell-type level. Single-cell RNA-sequencing (scRNA-seq) has made feasible the profiling of the transcriptome of a single cell. Consequently, the scRNA-seq data of four KIRC patients were analyzed. A total of four KIRC patients undergoing radical nephrectomy provided a total of eight tissue samples for this investigation. The Materials and methods section describes the quality control criteria. A total of five separate clusters with diverse gene profiles were identified using unsupervised clustering of these cells and their distributions were comparable across patients (Fig. 4A). After removing batch effects and regressing out the influence of the number of unique molecular identifiers (UMIs) and percentage of mitochondrion-derived UMI counts, 9,333 cells with ≥200 UMIs passed the quality filtering. These cells were separated into six major cell lineages: B cells, CD8 T cells, endothelium cells, epithelial cells, macrophage cells and smooth muscle cells (Fig. 4B). The annotation of various clusters in Fig. 4C was performed in accordance with the type of tissue sample. In different cases, the boundaries between neighboring benight tumor tissue cells are unclear, although tumor tissue cells are relatively autonomous (Fig. 4C). Fig. 4D is a dot diagram illustrating marker genes for each cell subgroup.

The present study estimated and identified large-scale chromosomal CNV by inferCNV for each sample based on transcriptomes to identify malignant cells. Epithelial cells from tumor tissues generated an inferCNV clustered heatmap that matches to the normalized expression levels of epithelial

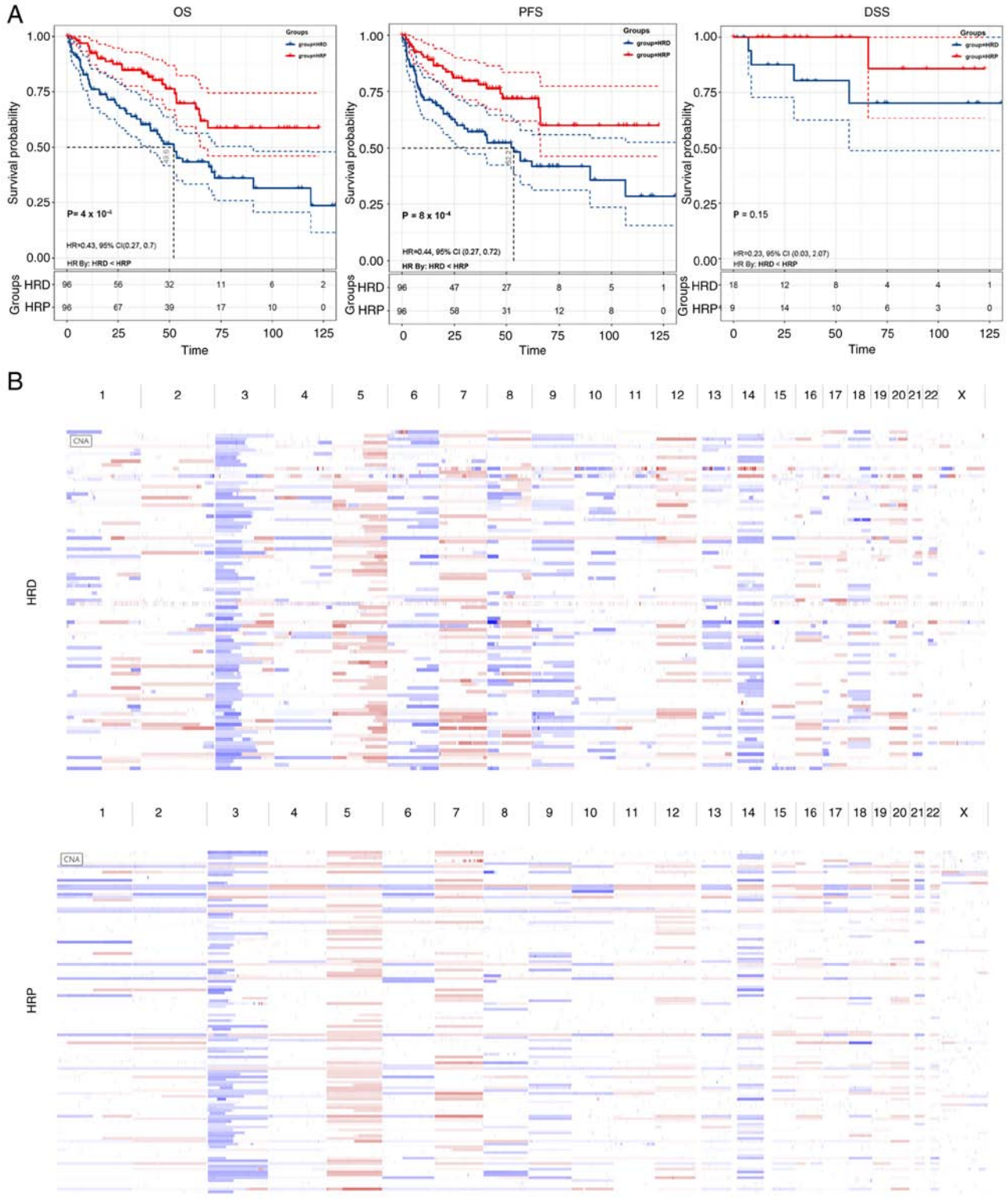

Figure 1. The clinical significance of HRD in the TCGA-KIRC cohort. (A) Kaplan-Meier analysis of survival revealed OS, PFS and DSS differences between HRD and HRP patients in the TCGA-KIRC cohort. (B) Genome-wide copy number variation analysis revealed genomic instability differences between HRD and HRP patients. HRD, homologous recombination deficit; TCGA, The Cancer Genome Atlas; KIRC, kidney renal clear cell carcinoma; HRP, homologous recombination proficient; OS, overall survival; PFS, progression-free survival; DSS, disease-specific survival.

cells in benight neighboring tumor tissue. The resultant CNV heatmap depicted regions of increase in red and regions of loss in blue. As there were not enough epithelial cells in some samples, epithelial cells from the normal tissues of patients 2 and 3 were chosen as the control group and the tumor tissues of patients 1 and 4 were chosen as the case group. It was discovered that the epithelial cells of tumor tissues underwent significant CNV occurrences compared with control cells (Fig. 5A). These findings indicated that the epithelial cells were cancerous cells. Compared with conventional bulk RNA-seq, scRNA-seq may assess TME with greater precision. Therefore, KEGG enrichment analysis was conducted

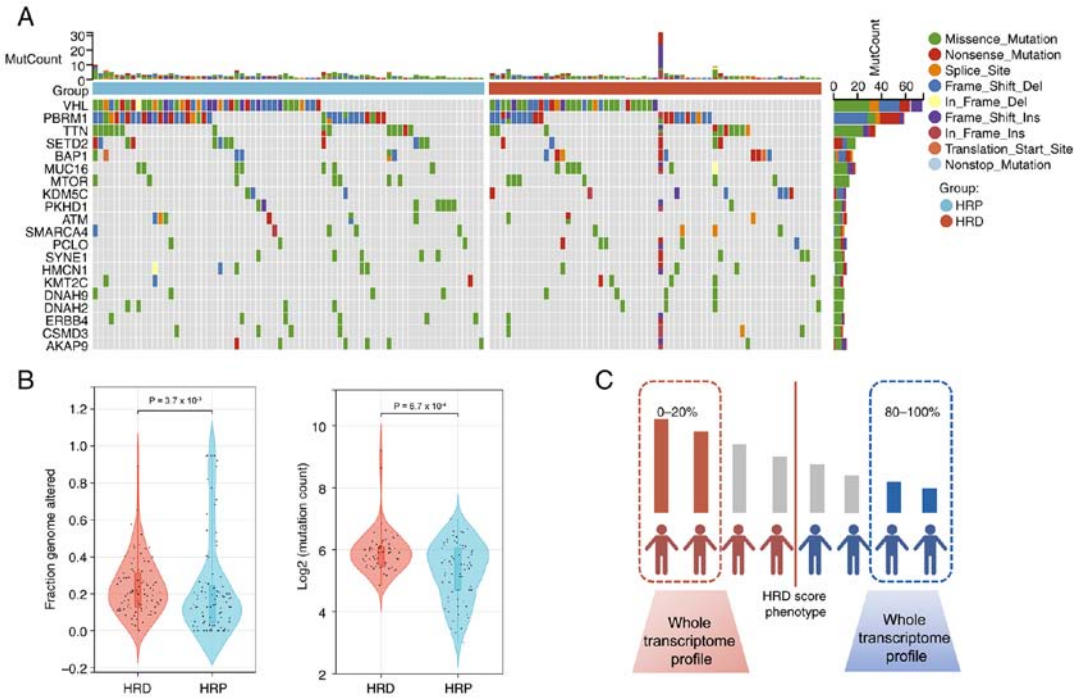

Figure 2. The mutation landscape in the TCGA-KIRC cohort. (A) Summary of the most prevalent genomic alterations in different HRD group. The mutational matrix shows Missense_Mutations (green), Nonsense_Mutations (red), Frame_shift_Deletions (blue), Splice_site mutations (orange), Frame_shift_Insertions (purple), In_Frame_Dels (yellow), In_Frame_Ins (brownness), Translation_Start_Site mutations (light brown), Nonstop_Mutations (light blue). (B) Violin plot of fraction of genome altered in HRD and HRP groups (Wilcoxon signed-rank test;); Violin plot of mutation count in the HRD and the HRP groups (Wilcoxon signed-rank test;). (C) WES calculated HRD scores for each KIRC patient, with the 20% of patients with the highest HRD scores constituting the HRD group and the 20% of patients with the lowest HRD scores constituting the HRP group. TCGA, The Cancer Genome Atlas; KIRC, kidney renal clear cell carcinoma; HRD, homologous recombination deficit; HRP, homologous recombination proficient; WES, whole exome sequencing.

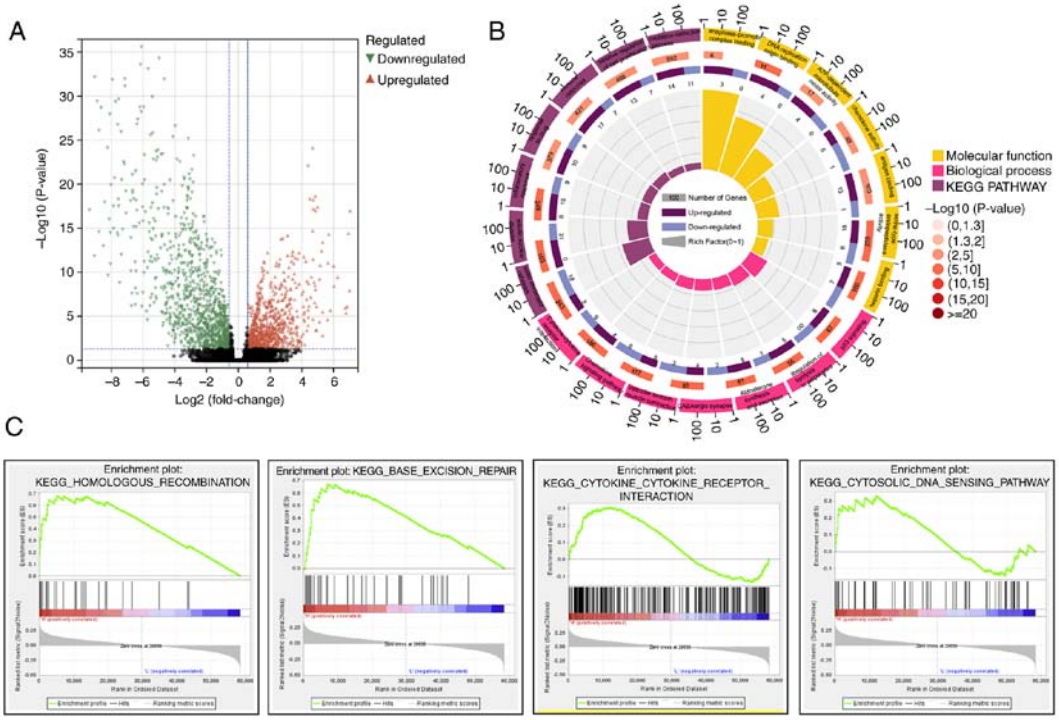

Figure 3. Analysis of the transcriptome profiles of patients with HRD and HRP. (A) DEGs between HRD and HRP subtypes. The red triangles represent differentially upregulated genes, whereas the green triangles represent differentially downregulated genes. (B) GO term and KEGG analysis of upregulated pathways in the HRD group compared with the HRP group was conducted. The first lap indicates the top 21 GO terms and the outer lap corresponds to the number of genes. The second lap specifies the number of genes in the genome background as well as the Q values for enrichment of upregulated genes for the specified biological process. The third lap indicates the ratio of upregulated (dark purple) to downregulated (light purple) genes. The fourth lap represents the enrichment factor of each GO term. (C) GSEA of the most enriched pathways of the HRD group compared with the HRP group. HRD, homologous recombination deficit; HRP, homologous recombination proficient; DEGs, differentially expressed genes; GO. gene ontology; KEGG, Kyoto Encyclopedia of Genes and Genomes; GSEA, gene set enrichment analysis.

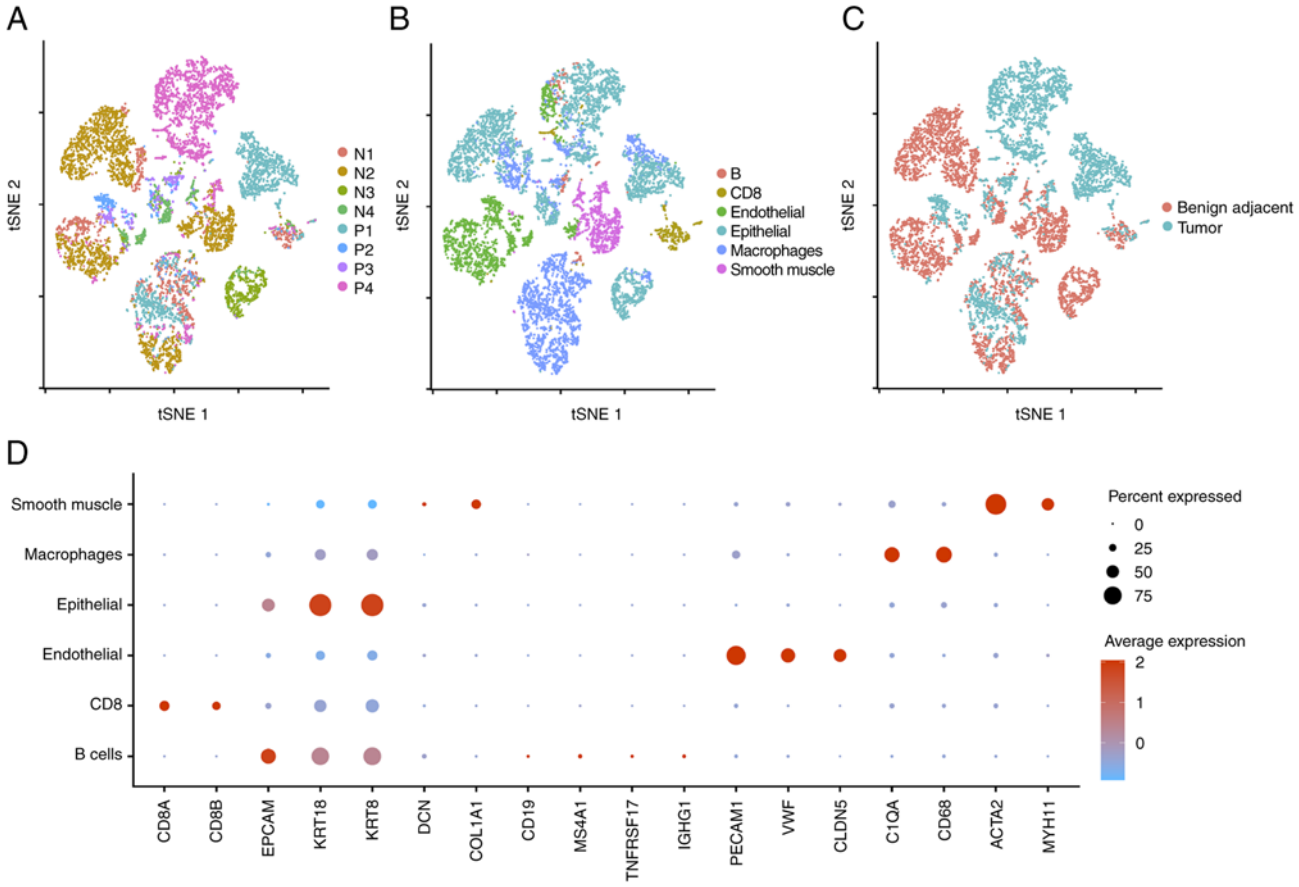

Figure 4. Single-cell sequencing analysis of tissue samples from HRD-positive KIRC patients. (A) tSNE embedding of tumor and adjacent noncancerous cell transcriptional profiles in four patients. Each dot represents a single cell, while each color corresponds to a distinct sample. (B) tSNE plot of the six major cell types identified in tumors and their adjacent tissues. (C) The type of tissue sample is taken into consideration while annotating the different clusters in tSNE plot. (D) Bubble diagram displaying signature gene expressions across the six cellular clusters. The size of the dots indicates the proportion of cells that express a particular marker, while the color indicates the average expression levels of the markers. HRD, homologous recombination deficit; KIRC, kidney renal clear cell carcinoma; tSNE, t-distributed stochastic neighbor embedding; N, para-carcinoma tissue; P, tumor tissue.

on the upregulated and downregulated DEGs of malignant and normal epithelial cells. As indicated in Fig. 5B, epithelial cells of tumor tissue were enriched in the DNA repair, cell cycle, Chemokine-Chemokine receptor interaction and innate immune response pathways.

Analysis of the T cell characteristics of HRD-positive KIRC patients using single-cell sequencing. Chemokine-related signaling pathways play a crucial role in the migration of T cells (34,35). The present study speculated that HRD-positive patients may be characterized by the presence of loss-of-function mutations in homologous recombination repair (HRR)-related genes, whereas patients with HRP may lack mutations in genes involved in the HRR signaling pathway. The present study found that in HRD-positive cancers, the chemokine-related signaling pathways were activated (Fig. 5B). To further characterize T cells in HRD tumors, the present study evaluated scRNA-seq data recovered from HRD and HRP tumor-infiltrating T lymphocyte suspensions . scType algorithm classified T cells as $CD8^+$ (ISG+, NME1+, Tex and Trm) and CD4+ regulatory (Fig. 5C). Expression of cytotoxicity marker genes, such as GZMA/B/K and IFNG and immunological checkpoint marker genes, such as LAG3 and PDCD1, distinguished $CD8^+$ Tex cells (Fig. 5D). The percentage of lymphocytes infiltrating HRD and HRP tumors were then compared. As depicted in Fig. 5E, when HRD tumors were compared with HRP cancers, $CD8^+$ Tex cells were dramatically increased (60% vs. 6.2%, $P<0.001$) and CD4 + regulatory cells were significantly decreased (0.1 percent vs. 17.2%, $P<0.001$).

Discussion

Malignancies frequently exhibit HRD, a common genetic abnormality (36). The improvement of our understanding of malignancies is facilitated by HRD research. Despite the fact that few research have addressed the impact and importance of HRD in KIRC, genomic instability is associated to the prevalence of the disease (37,38). While KIRC has additional genomic instability characteristics, it has a lower prevalence of BRCA1/2 mutations than breast or ovarian cancer. Additionally, KIRC had not offered a gene panel gold standard for HRD detection. A mutational signature-based technique for predicting HRD is the HRD score. It can more correctly predict HRD in KIRC since it focuses on the consequences of HRD rather than its root cause. The present study was the first to look into the prognostic value of HRD in KIRC, to the best of the authors' knowledge.

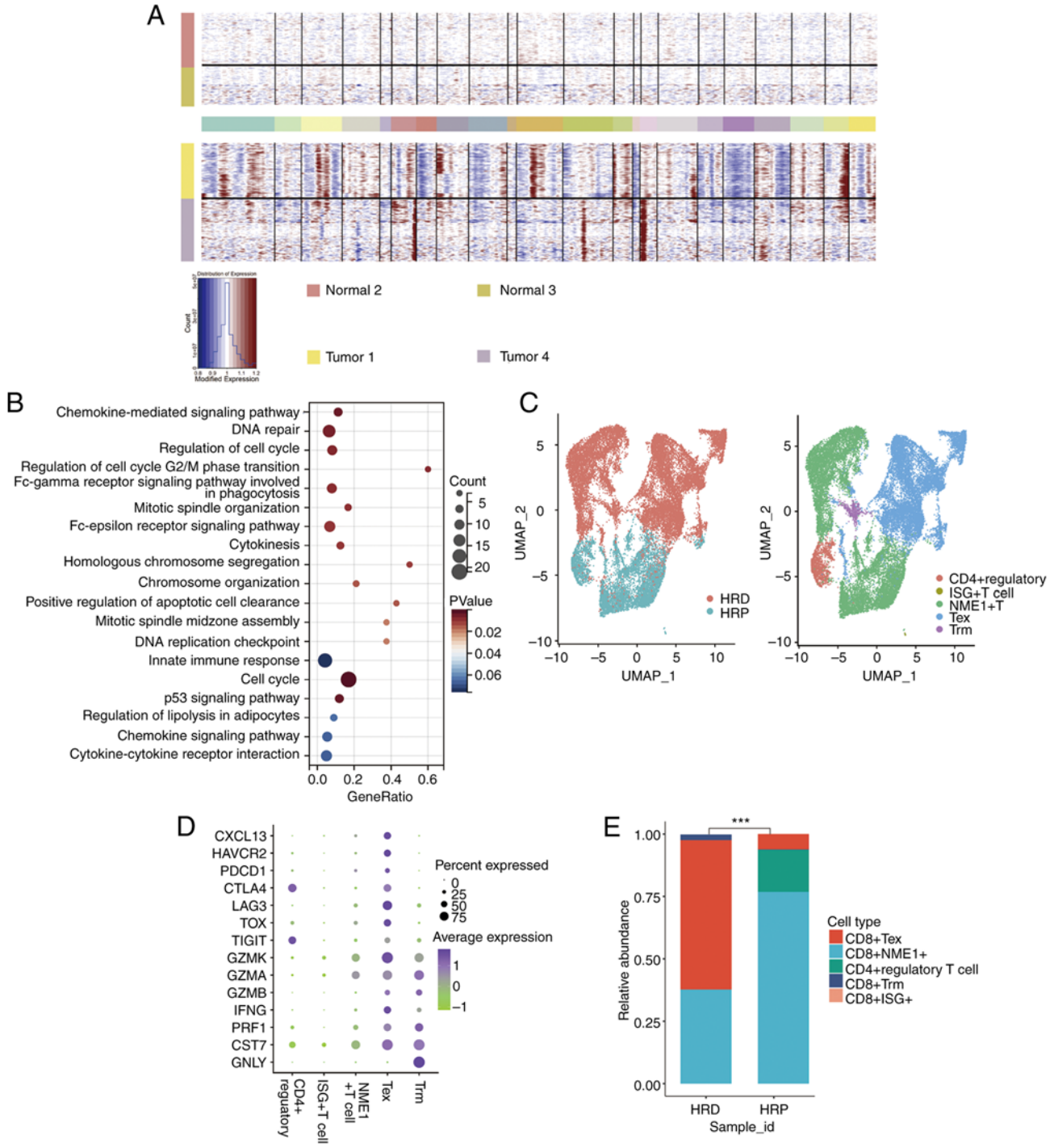

Figure 5. Single-cell sequencing analysis of the T-cell characteristics of HRD-positive KIRC patients. (A) Top, the hierarchical heatmap displaying large-scale CNVs in normal tissues from the epithelial cells of two KIRC patients; bottom, the hierarchical heatmap displaying large-scale CNVs in tumor tissues from the epithelial cells of two KIRC patients. (B) Analysis of differential genes in malignant epithelial cells based on KEGG and GO functional enrichment. (C) Left, UMAP projection of cells colored by HRD and HRP patients. Right, the tSNE plot of the five major T cell types isolated from tumor tissues. (D) The bubble chart displays the 14 signature gene expressions across the five cellular clusters. The size of the dots represents the percentage of cells that express a particular marker and the color spectrum indicates the average expression levels of the markers (log1p transformed). (E) Relative proportion of each cell cluster from HRD and HRP patients as indicated. ***P<0.01. HRD, homologous recombination deficit; KIRC, kidney renal clear cell carcinoma; CNVs, single-cell copy-number variation; KEGG, Kyoto Encyclopedia of Genes and Genomes; UMAP, uniform manifold approximation and projection; HRP, homologous recombination proficient; tSNE, t-distributed stochastic neighbor embedding.

Patients with KIRC frequently experience recurring tumors as distant metastases and only 10% of them respond to chemotherapy (5). This may be due to the absence of biomarkers that stratify chemotherapy treatment and HRD may be an excellent biomarker for predicting the efficacy of platinum treatment in KIRC. Obviously, additional research is required to determine the relationship between HRD-positive KIRC patients and the efficacy of platinum treatment.

By analyzing the expression profile of patients with different HRD scores, the present study identified DNA

damage repair (DDR) signaling pathways and the innate immune related pathways were enriched in patients with high HRD scores. The widespread activation of DDR signaling pathways supports the notion that HRD serves as a biomarker for assessing genomic instability (39). Additionally, HRD patients exhibit activation of innate immune-related signaling pathways. To confirm that these activated immune-related signaling pathways originate from HRD tumor cells, the present study conducted scRNA-seq analyses. The results of scRNA-seq directly proved that HRD tumor cells upregulated the Chemokine-related signaling pathways. Chemokines are a class of proteins that attract leukocytes to the site of infection and serve an important role in the inflammatory response (40). Researchers believe that chemokines also play a key role in tumorigenesis and development. For example, some studies have found that chemokines mediate a variety of immune cells into the tumor microenvironment, help T cells enter tumors and affect tumor immunity and therapeutic effects (40-42). The activation of Chemokine-related signals causes changes in TME (37), as evidenced by scRNA-seq results of T lymphocytes: intratumoral T cells in the HRD patients were distinct from T cells in the HRP patients. The present study found that KIRC patients with HRD had the highest proportion of *CXCL13*$^{+}$ Tex. Previous studies have shown that *CXCL13* is a signature gene of tumor-specific T cells (43,44) and these results suggest that KIRC patients with HRD may have a higher proportion of tumor-specific T lymphocytes in their tumors and that immunotherapy may benefit these patients. Furthermore, the present study discovered that intratumoral T cells in HRP had a larger percentage of Treg cells. Further investigation is necessary to determine the cause of this event.

It was expected that the results of the present study will provide important insights and lead to a more effective therapeutic treatment and prognosis for KIRC. As the present study was conducted on a cohort from a public database, it did not collect comprehensive clinical data regarding the clinical care of patients and treatment options. More research is needed on the prognostic mechanism of genomic instability in KIRC. The analysis and discussion of the HRD-related genome, transcriptome and TME in this review would provide a new method for identifying therapy- and prognosis-related biomarkers.

Acknowledgements

Not applicable.

Funding

The present study was funded by Key Medical Discipline of Hangzhou City (grant no. 2021-21), Key Medical Discipline of Zhejiang Province (grant no. 2018-2-3) and Key Laboratory of Clinical Cancer Pharmacology and Toxicology Research of Zhejiang Province (grant no. 2020E10021).

Availability of data and materials

The single cell datasets and code generated during the present study this investigation are accessible in the Zenodo database (https://zenodo.org/record/7783618#.ZCTwZXZBy3A).

Authors' contributions

LH, FG, JZ and QX designed the present study. YH and LH collected data. FG, MY and QY analyzed data. YH, QX, MY and JZ prepared the manuscript and MY and QY checked the grammar. YH and LH supervised the present study. YH was responsible for funding acquisition. YH and LH confirm the authenticity of all the raw data. All authors read and approved the final manuscript.

Ethics approval and consent to participate.

Experiments with human participants were approved by the Research Ethics Committee of Hangzhou Hospital of Traditional Chinese Medicine (approval number: 2019KY005) and performed according to the Declaration of Helsinki.

Patient consent for publication

Not applicable.

Competing interests

The authors declare that they have no competing interests.

References

1. Hsieh JJ, Purdue MP, Signoretti S, Swanton C, Albiges L, Schmidinger M, Heng DY, Larkin J and Ficarra V: Renal cell carcinoma. Nat Rev Dis Primers 3: 17009, 2017.
2. Sanchez DJ and Simon MC: Genetic and metabolic hallmarks of clear cell renal cell carcinoma. Biochim Biophys Acta Rev Cancer 1870: 23-31, 2018.
3. Lobo J, Ohashi R, Amin MB, Berney DM, Compérat EM, Cree IA, Gill AJ, Hartmann A, Menon S, Netto GJ, *et al*: The WHO 2022 landscape of papillary and chromophobe renal cell carcinoma. Histopathology 81: 426-438, 2022.
4. Choueiri TK and Motzer RJ: Systemic therapy for metastatic renal-cell carcinoma. N Eng J Med 376: 354-366, 2017.
5. Makhov P, Joshi S, Ghatalia P, Kutikov A, Uzzo RG and Kolenko VM: Resistance to systemic therapies in clear cell renal cell carcinoma: Mechanisms and management strategies. Mol Cancer Ther 17: 1355-1364, 2018.
6. Hsieh JJ, Le VH, Oyama T, Ricketts CJ, Ho TH and Cheng EH: Chromosome 3p loss-orchestrated VHL, HIF and epigenetic deregulation in clear cell renal cell carcinoma. J Clin Oncol 36: JCO2018792549, 2018.
7. Liao L, Liu ZZ, Langbein L, Cai W, Cho EA, Na J, Niu X, Jiang W, Zhong Z, Cai WL, *et al*: Multiple tumor suppressors regulate a HIF-dependent negative feedback loop via ISGF3 in human clear cell renal cancer. Elife 7: e37925, 2018.
8. De Cubas AA and Rathmell WK: Epigenetic modifiers: Activities in renal cell carcinoma. Nat Rev Urol 15: 599-614, 2018.
9. Ledermann JA, Drew Y and Kristeleit RS: Homologous recombination deficiency and ovarian cancer. Eur J Cancer 60: 49-58, 2016.
10. Shi Z, Zhao Q, Lv B, Qu X, Han X, Wang H, Qiu J and Hua K: Identification of biomarkers complementary to homologous recombination deficiency for improving the clinical outcome of ovarian serous cystadenocarcinoma. Clin Transl Med 11: e399, 2021.
11. Marquard AM, Eklund AC, Joshi T, Krzystanek M, Favero F, Wang ZC, Richardson AL, Silver DP, Szallasi Z and Birkbak NJ: Pan-cancer analysis of genomic scar signatures associated with homologous recombination deficiency suggests novel indications for existing cancer drugs. Biomark Res 3: 1-10, 2015.
12. Telli ML, Timms KM, Reid J, Hennessy B, Mills GB, Jensen KC, Szallasi Z, Barry WT, Winer EP, Tung NM, *et al*: Homologous recombination deficiency (HRD) score predicts response to platinum-containing neoadjuvant chemotherapy in patients with triple-negative breast cancerHRD predicts response to platinum therapy in TNBC. Clin Cancer Res 22: 3764-3773, 2016.

13. Sztupinszki Z, Diossy M, Krzystanek M, Reiniger L, Csabai I, Favero F, Birkbak NJ, Eklund AC, Syed A and Szallasi Z: Migrating the SNP array-based homologous recombination deficiency measures to next generation sequencing data of breast cancer. NPJ Breast Cancer 4: 16, 2018.
14. Takaya H, Nakai H, Takamatsu S, Mandai M and Matsumura N: Homologous recombination deficiency status-based classification of high-grade serous ovarian carcinoma. Sci Rep 10: 2757, 2020.
15. Timms KM, Abkevich V, Hughes E, Neff C, Reid J, Morris B, Kalva S, Potter J, Tran TV, Chen J, *et al*: Association of BRCA1/2 defects with genomic scores predictive of DNA damage repair deficiency among breast cancer subtypes. Breast Cancer Res 16: 475, 2014.
16. Shi Z, Shen J, Qiu J, Zhao Q, Hua K and Wang H: CXCL10 potentiates immune checkpoint blockade therapy in homologous recombination-deficient tumors. Theranostics 11: 7175, 2021.
17. Merino DM, McShane LM, Fabrizio D, Funari V, Chen SJ, White JR, Wenz P, Baden J, Barrett JC, Chaudhary R, *et al*: Establishing guidelines to harmonize tumor mutational burden (TMB): In silico assessment of variation in TMB quantification across diagnostic platforms: Phase I of the friends of cancer research TMB harmonization project. J Immunother Cancer 8: e000147, 2020.
18. Gainor JF, Rizvi H, Jimenez Aguilar E, Skoulidis F, Yeap BY, Naidoo J, Khosrowjerdi S, Mooradian M, Lydon C, Illei P, *et al*: Clinical activity of programmed cell death 1 (PD-1) blockade in never, light and heavy smokers with non-small-cell lung cancer and PD-L1 expression ≥ 50%. Ann Oncol 31: 404-411, 2020.
19. Niu B, Ye K, Zhang Q, Lu C, Xie M, McLellan MD, Wendl MC and Ding L: MSIsensor: microsatellite instability detection using paired tumor-normal sequence data. Bioinformatics 30: 1015-1016, 2014.
20. Tomczak K, Czerwińska P and Wiznerowicz M: Review the cancer genome atlas (TCGA): An immeasurable source of knowledge. Contemp Oncol (Pozn) 2015: A68-A77, 2015.
21. Koboldt DC, Zhang Q, Larson DE, Shen D, McLellan MD, Lin L, Miller CA, Mardis ER, Ding L and Wilson RK: VarScan 2: Somatic mutation and copy number alteration discovery in cancer by exome sequencing. Genome Res 22: 568-576, 2012.
22. Wang K, Li M and Hakonarson H: ANNOVAR: Functional annotation of genetic variants from high-throughput sequencing data. Nucleic Acids Res 38: e164, 2010.
23. Gao J, Aksoy BA, Dogrusoz U, Dresdner G, Gross B, Sumer SO, Sun Y, Jacobsen A, Sinha R, Larsson E, *et al*: Integrative analysis of complex cancer genomics and clinical profiles using the cBioPortal. Sci Signal 6: pl1, 2013.
24. Au L, Hatipoglu E, Robert de Massy M, Litchfield K, Beattie G, Rowan A, Schnidrig D, Thompson R, Byrne F, Horswell S, *et al*: Determinants of anti-PD-1 response and resistance in clear cell renal cell carcinoma. Cancer Cell 39: 1497-1518.e11, 2021.
25. Abkevich V, Timms KM, Hennessy BT, Potter J, Carey MS, Meyer LA, Smith-McCune K, Broaddus R, Lu KH, Chen J, *et al*: Patterns of genomic loss of heterozygosity predict homologous recombination repair defects in epithelial ovarian cancer. Br J Cancer 107: 1776-1782, 2012.
26. Popova T, Manié E, Rieunier G, Caux-Moncoutier V, Tirapo C, Dubois T, Delattre O, Sigal-Zafrani B, Bollet M, Longy M, *et al*: Ploidy and large-scale genomic instability consistently identify basal-like breast carcinomas with BRCA1/2 inactivation. Cancer Res 72: 5454-5462, 2012.
27. Birkbak NJ, Wang ZC, Kim JY, Eklund AC, Li Q, Tian R, Bowman-Colin C, Li Y, Greene-Colozzi A, Iglehart JD, *et al*: Telomeric allelic imbalance indicates defective DNA repair and sensitivity to DNA-damaging agents. Cancer Discov 2: 366-375, 2012.
28. Love MI, Huber W and Anders S: Moderated estimation of fold change and dispersion for RNA-seq data with DESeq2. Genome Biol 15: 550, 2014.
29. Subramanian A, Tamayo P, Mootha VK, Mukherjee S, Ebert BL, Gillette MA, Paulovich A, Pomeroy SL, Golub TR, Lander ES and Mesirov JP: Gene set enrichment analysis: A knowledge-based approach for interpreting genome-wide expression profiles. Proc Natl Acad Sci USA 102: 15545-15550, 2005.
30. McGinnis CS, Murrow LM and Gartner ZJ: DoubletFinder: Doublet detection in single-cell RNA sequencing data using artificial nearest neighbors. Cell Syst 8: 329-337.e4, 2019.
31. Korsunsky I, Millard N, Fan J, Slowikowski K, Zhang F, Wei K, Baglaenko Y, Brenner M, Loh PR and Raychaudhuri S: Fast, sensitive and accurate integration of single-cell data with Harmony. Nat Methods 16: 1289-1296, 2019.
32. Ianevski A, Giri AK and Aittokallio T: Fully-automated and ultra-fast cell-type identification using specific marker combinations from single-cell transcriptomic data. Nature Commun 13: 1246, 2022.
33. Li X and Wang CY: From bulk, single-cell to spatial RNA sequencing. Int J Oral Sci 13: 36, 2021.
34. Poznansky MC, Olszak IT, Foxall R, Evans RH, Luster AD and Scadden DT: Active movement of T cells away from a chemokine. Nat Med 6: 543-548, 2000.
35. Greener JG, Kandathil SM, Moffat L and Jones DT: A guide to machine learning for biologists. Nat Rev Mol Cell Biol 23: 40-55, 2022.
36. Alhmoud JF, Woolley JF, Al Moustafa AE and Malki MI: DNA damage/repair management in cancers. Cancers (Basel) 12: 1050, 2020.
37. Wang Y, Yan K, Wang L and Bi J: Genome instability-related long non-coding RNA in clear renal cell carcinoma determined using computational biology. BMC Cancer 21: 1-13, 2021.
38. Niu S, Liu K, Xu Y, et al.: Genomic landscape of Chinese clear cell renal cell carcinoma patients with venous tumor thrombus identifies chromosome 9 and 14 deletions and related immunosuppressive microenvironment. Front Oncol 11: 646338, 2021.
39. Fakouri NB, Hou Y, Demarest TG, Christiansen LS, Okur MN, Mohanty JG, Croteau DL and Bohr VA: Toward understanding genomic instability, mitochondrial dysfunction and aging. FEBS J 286: 1058-1073, 2019.
40. Kohli K, Pillarisetty VG and Kim TS: Key chemokines direct migration of immune cells in solid tumors. Cancer Gene Ther 29: 10-21, 2022.
41. Dangaj D, Bruand M, Grimm AJ, Ronet C, Barras D, Duttagupta PA, Lanitis E, Duraiswamy J, Tanyi JL, Benencia F, *et al*: Cooperation between constitutive and inducible chemokines enables T cell engraftment and immune attack in solid tumors. Cancer Cell 35: 885-900.e10, 2019.
42. Mollica Poeta V, Massara M, Capucetti A and Bonecchi R: Chemokines and chemokine receptors: New targets for cancer immunotherapy. Front Immunol 10: 379, 2019.
43. Lowery FJ, Krishna S, Yossef R, Parikh NB, Chatani PD, Zacharakis N, Parkhurst MR, Levin N, Sindiri S, Sachs A, *et al*: Molecular signatures of antitumor neoantigen-reactive T cells from metastatic human cancers. Science 375: 877-884, 2022.
44. Zheng C, Fass JN, Shih YP, Gunderson AJ, Sanjuan Silva N, Huang H, Bernard BM, Rajamanickam V, Slagel J, Bifulco CB, *et al*: Transcriptomic profiles of neoantigen-reactive T cells in human gastrointestinal cancers. Cancer Cell 40: 410-423.e17, 2022.